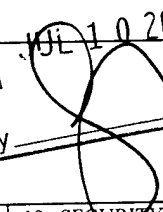


REPORT DOCUMENTATION PAGE

Form Approved
OMB NO. 0704-0188

Public Reporting burden for this collection of information is estimated to average 1 hour per response, including the time for reviewing instructions, searching existing data sources, gathering and maintaining the data needed, and completing and reviewing the collection of information. Send comment regarding this burden estimate or any other aspect of this collection of information, including suggestions for reducing this burden, to Washington Headquarters Services, Directorate for Information Operations and Reports, 1215 Jefferson Davis Highway, Suite 1204, Arlington, VA 22202-4302, and to the Office of Management and Budget, Paperwork Reduction Project (0704-0188), Washington, DC 20503.

1. AGENCY USE ONLY (Leave Blank)		2. REPORT DATE June 26, 2001	3. REPORT TYPE AND DATES COVERED Final Progress Report/June 1, 1999 - October 31, 2000 31 Aug 00	
4. TITLE AND SUBTITLE A fundamental investigation into the deformation and failure behavior of heterogeneous materials with the aim of developing design guidelines			5. FUNDING NUMBERS DAAD 19-99-1-0224	
6. AUTHOR(S) Krishnaswamy RAVI-CHANDAR			8. PERFORMING ORGANIZATION REPORT NUMBER	
7. PERFORMING ORGANIZATION NAME(S) AND ADDRESS(ES) Department of Mechanical Engineering University of Houston Houston, TX 77204-4792			10. SPONSORING / MONITORING AGENCY REPORT NUMBER DAAD 19-99-1-0224 39794.1-EG	
9. SPONSORING / MONITORING AGENCY NAME(S) AND ADDRESS(ES) U. S. Army Research Office P.O. Box 12211 Research Triangle Park, NC 27709-2211			11. SUPPLEMENTARY NOTES The views, opinions and/or findings contained in this report are those of the author(s) and should not be construed as an official Department of the Army position, policy or decision, unless so designated by other documentation.	
12 a. DISTRIBUTION / AVAILABILITY STATEMENT Approved for public release; distribution unlimited.			12 b. DISTRIBUTION CODE	
13. ABSTRACT (Maximum 200 words) The objective of the work is to investigate the mechanisms of load transfer, deformation and failure in composites under multiaxial loading in order to link the heterogeneity and anisotropy at the microscale to the macroscale design of composite structures. This is important since the deformation and failure behavior under multiaxial is not well understood, nor are there suitable design guidelines or material allowables clearly defined. Careful experiments have been designed to examine these issues. In these experiments, in addition to measurements of the global behavior of the composites, local variations in the deformation are obtained through digital image correlation. Digital image correlation technique is based on comparing a digital image before and after deformation and extracting the displacements and strains by minimizing a correlation function. This method has been implemented and demonstrated its capabilities by experimenting with a polycarbonate specimen. Local mechanical properties of the constituents are also measured. For example it was found that by applying a confining pressure under multiaxial constraint, the flow resistance for polyetheretherketone (PEEK), can be increased significantly. The Principal Investigator moved to the University of Texas at Austin before the completion of the project at the University; the grant was terminated and reissued to UT Austin; experiments on unidirectional composite specimens will be performed at the University of Texas at Austin over the next two years.				
14. SUBJECT TERMS			15. NUMBER OF PAGES 12	
17. SECURITY CLASSIFICATION OR REPORT UNCLASSIFIED			16. PRICE CODE	
18. SECURITY CLASSIFICATION ON THIS PAGE UNCLASSIFIED		19. SECURITY CLASSIFICATION OF ABSTRACT UNCLASSIFIED		20. LIMITATION OF ABSTRACT UL

RECEIVED
 JUN 10 2001
 By: 

FOREWORD

This report describes work aimed at investigating the behavior of composites under multiaxial loading. Work on the project began at the University of Houston. Experiments to determine local variations of deformation and local mechanical properties have been developed and demonstrated. In August 2000, the PI's accepted a faculty position and moved to the University of Texas at Austin. This resulted in an interruption of the project; the project was terminated at the University of Houston, and then reissued to the PI at the University of Texas at Austin. This process took about eight months to accomplish. In this report, the work done at the University of Houston is described. Further work on applying these methods to the examination of the deformation and failure of composites is currently underway at the University of Texas.

STATEMENT OF THE PROBLEM STUDIED

We believe that through an understanding of the micromechanical deformation and load transfer, design with composites can be approached by coupling the microstructural design and macrostructural design. This approach will eliminate the need for *ad hoc* strengths and provide for design using the fundamental material properties of the constituents. In order to develop this methodology, it is necessary to understand the deformation and failure behavior of composites at the level of the heterogeneity. This is the objective of the present work. We are examining a multiaxial loading condition as described in Figure 1. While most experiments focus on measurements at the global level, we combine these global measurements with measurements of the local variations of the deformation through a digital image correlation technique. Local mechanical properties are also necessary to implement these ideas. With a view towards establishing

20010725 017

this experimental strategy, we have two experimental schemes that are currently under development. First is a digital image correlation method for the measurement of displacements with a resolution of 20 microstrains over spatial domains that are on the order of a few hundred microns. The second is a technique for evaluating the properties of the constituent materials under multiaxial stress states similar to that experienced by the matrix material *in situ*.

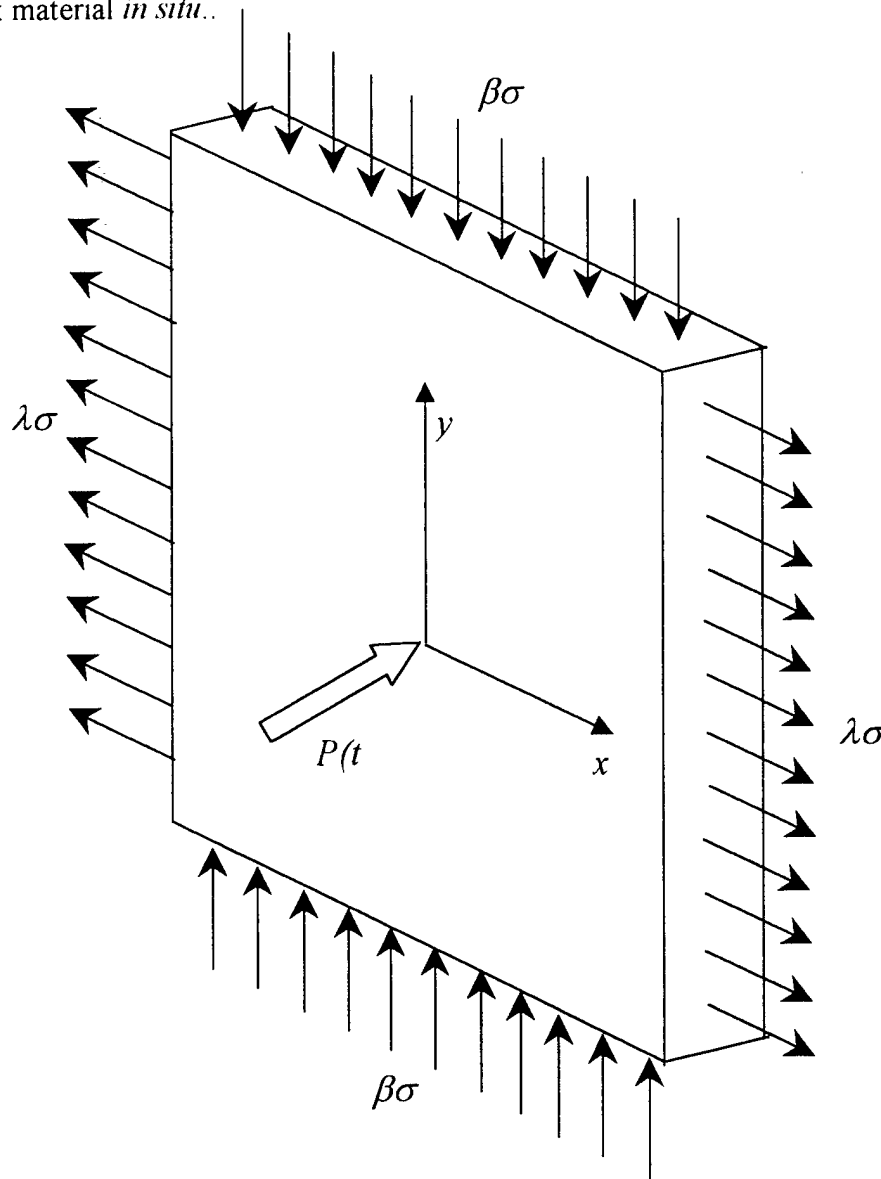


Figure 1. Macrostructural geometry and loading configuration. Multiaxial loading and out-of-plane deformations can be varied by varying the parameters in this configuration.

SUMMARY OF IMPORTANT RESULTS

We describe briefly the results obtained using the digital image correlation method and the confined compression scheme for multiaxial characterization of materials.

DIGITAL IMAGE CORRELATION

This method has been used by a number of investigators (for example, Peters and Ranson, 1980, Sutton *et al.*, 1991, Vendroux and Knauss, 1998) The principle of the method is illustrated in Figure 2, where the basic analytical element, the subset size is defined as a region of $\pm\Delta$ pixels around the reference point x_0 . A comparison of small subsets, centered at those reference points, yields local strain and displacement measurements at those pre-defined points. This is discussed in the following for one-dimensional deformations, the formulas are generally applicable for the three-dimensional case. Let $y=f(x)$ represent the deformation and let $A(x)$ and $B(y)$ define the intensity variations of the images, before and after deformation, respectively. We first define an array of points on the undeformed image where the displacements and strains will be computed. Then we define a subset S of the undeformed image around each of those reference points x_0 . To that subset is applied a function $f(x)$ that is supposed to 'model' the deformation, such that

$$f(x) = x + u(x_0) + \left(\frac{du}{dx} \right)_{x_0} (x - x_0) \quad (1)$$

The numerical intensity $A(x)$ of the undeformed image at points x of S are compared to the intensity $B(f(x))$ via a correlation coefficient C . The set of displacements $u(x_0)$ and strains $[du/dx]_{x_0}$ that minimize the correlation coefficient becomes the solution for the displacements and strains. The cross following correlation coefficients has been widely used:

$$C\left(u, \left(\frac{du}{dx} \right)\right) = \frac{\int_S A(x)B(f(x))dx}{\left[\int_S A(x)^2 dx \int_S B(f(x))^2 dx \right]^{1/2}} \quad (2)$$

with S such that $x \in S \Leftrightarrow (x_0 - \Delta) \leq x \leq (x_0 + \Delta)$

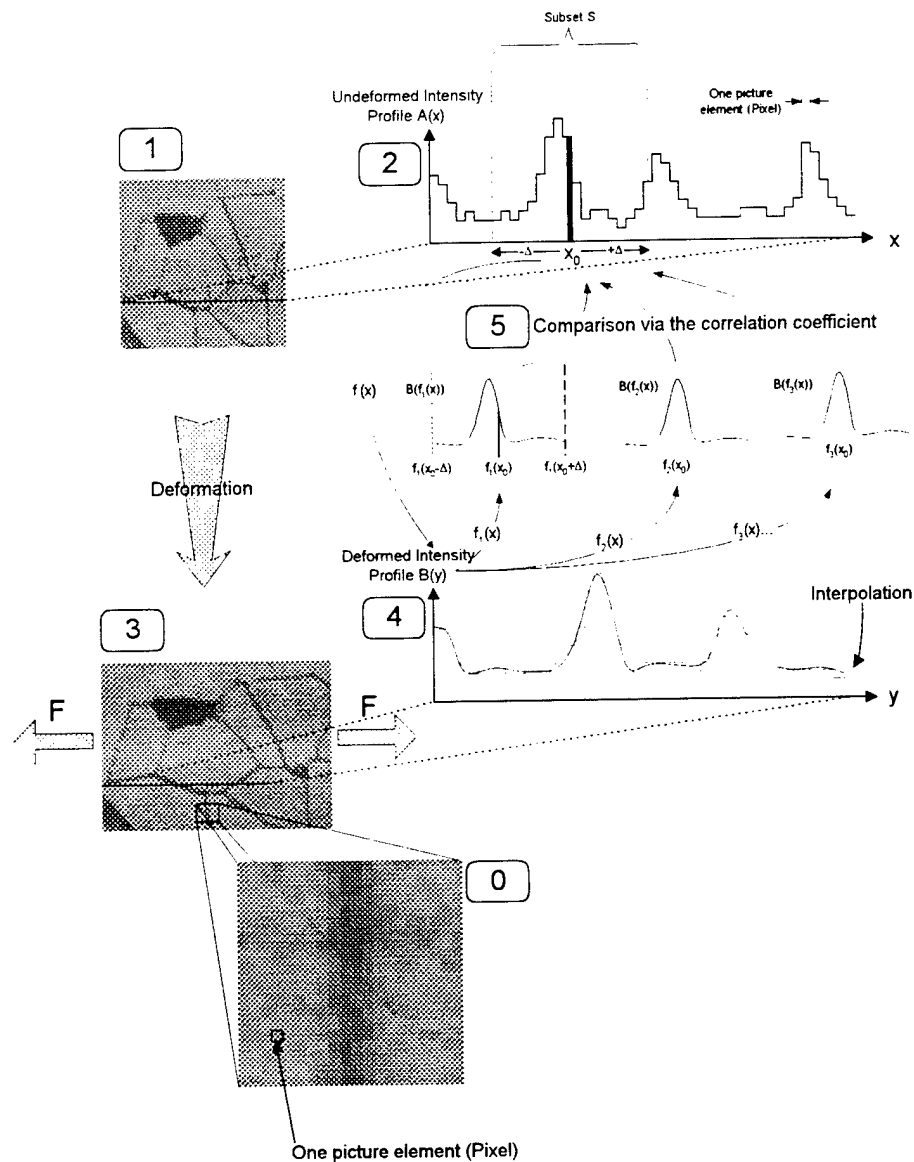


Figure 2: Principle of the Digital Image Correlation method - **0**: Detail of an image showing the decomposition in pixels - **1**: Picture of the undeformed microstructure - **2**: Spatial gray scale intensity variations $A(x)$ over a horizontal line of pixels of the undeformed image - **3**: Picture of the deformed microstructure under a tensile load F (the deformation is exaggerated for effect) - **4**: The dashed line shows the intensity variations $B(x)$ over the same line as in 2. The solid line represents the corresponding interpolated intensity profile - **5**: An assumed strain is applied to the subset S of 1 through the function $f_i(x)$. Its image through $B(f_i(x))$ is compared to the undeformed intensity profile $A(x)$ for various values of the strain $f_1(x), f_2(x)$ etc.

In order to get subpixel accuracy the subsets from the deformed images must be interpolated. The interpolation method has been shown to influence the accuracy of the results. Although increasing the subset size generally improves the quality of the comparison, the effect of averaging the strains over the subset and an increased CPU time

must also be considered. The successive comparison of the subsets involves an iterative method. The first method used was the trial and error method, where the subsets are compared over each point of a given area, sequentially reducing the size and the step of the search around the point of minimum correlation coefficient until the target accuracy was reached. This method is time consuming and later improvements yielded to the use of a gradient method (Newton-Raphson scheme) which considers the gradient of the correlation coefficient in order to accelerate convergence. Unfortunately this method can stall at local minima and hence miss the solution. The correlation coefficient must also be considered. Cross correlation coefficient has been commonly used but other coefficients, such as a least square coefficient gave better results. This coefficient can be written as follows

$$C = \frac{\int_s [A(x) - B(f(x))]^2 dx}{\int_s A(x)^2 dx} \quad (3)$$

The accuracy of determining the displacements by a the digital image correlation method was examined analytically and experimentally; these are fully documented in a manuscript under preparation (Fossier, Ravi-Chandar and White, 2001). Here, we show the capability with two figures, one illustrating the method in a ceramic and the other in a polymer. Extensions to composites are quite straightforward. Figure 3 shows the application of the method to an magnesium aluminate spinel sample; a microtensile sample was loaded and viewed under a microscope; a surface coating was provided to enhance the DIC method. The elastic behavior under small loads (within a single grain) and the Poisson's ratio (also within a single grain) were measured. Clearly the DIC method provides measurements of mechanical properties at the scale of a grain. Figure 4 shows strain contours obtained for a polycarbonate sample in a three-point bend loading over a field of view of 800 μm x 800 μm ; while the global measurement of strain is uniform, the local measurement indicates significant nonuniformity. The nonuniformity of the strain distribution is evident in this figure and is a result of structural nonuniformity. These examples were a part of our initial studies to make sure that the image correlation method was appropriate for the task of determining local strain distributions in a composite specimen.

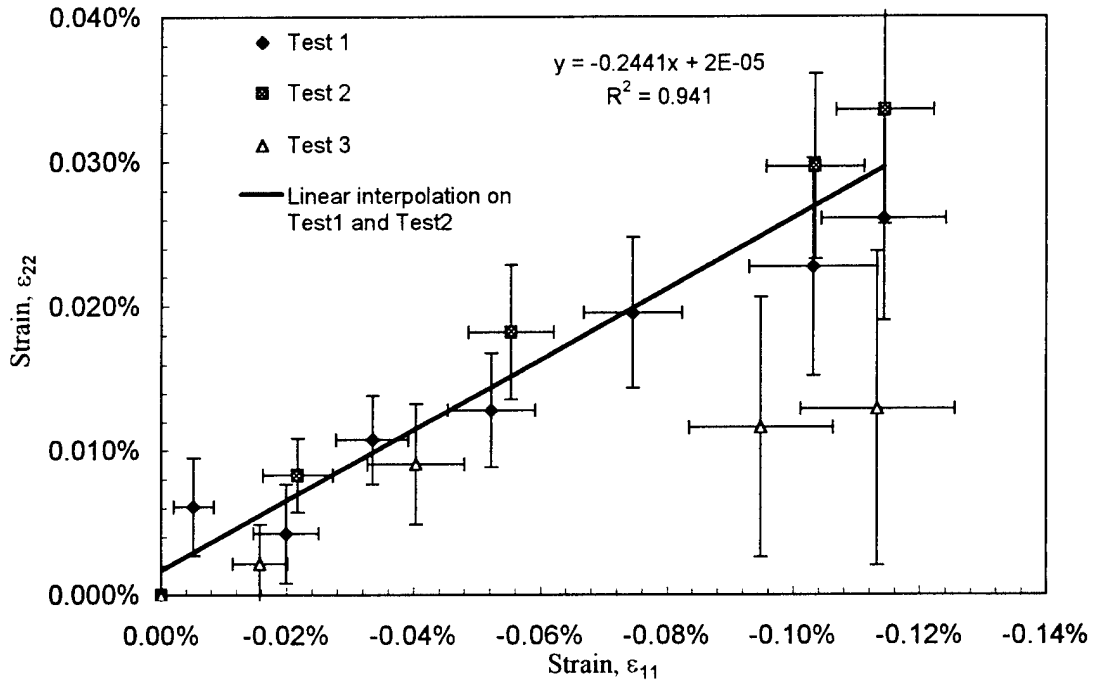
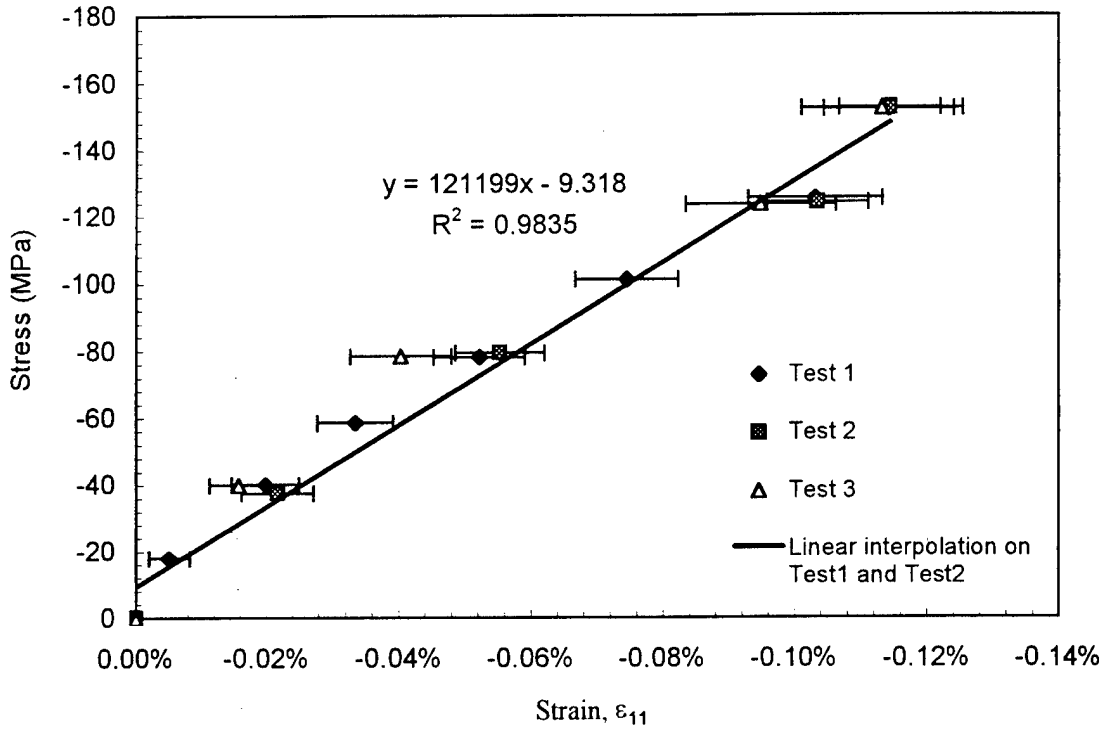


Figure 3: (a) Stress strain curve of a spinel single grain . (b) Strain in the direction of the loading axis against the strain perpendicular to the axis, showing the Poisson's ratio effect

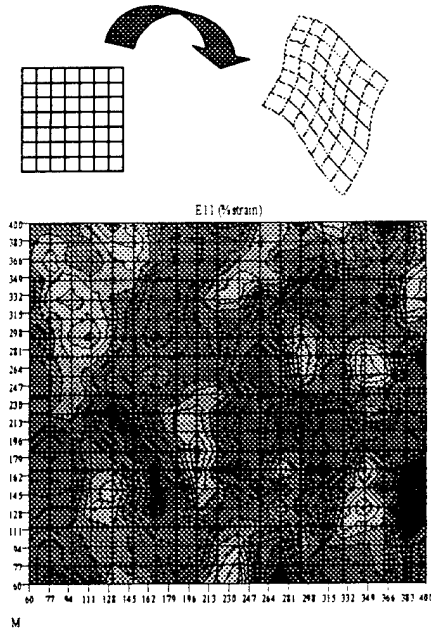


Figure 4. Strain distribution in a polycarbonate specimen under three point bending. Contours indicate constant strain levels. Obtained using digital image correlation

MULTIAXIAL MECHANICAL PROPERTIES

In the composite, the constituents are under multiaxial loading conditions even when the global loading is a simple uniaxial loading. In order to determine the actual local mechanical behavior, we have developed the confining cylinder experiment shown in Figure 5. The specimen is a cylindrical rod of diameter $2a$ and length L . It is inserted into the cavity of a hollow cylinder of internal diameter $2a$ and outer diameter $2b$; ideally the clearance between the specimen and the confining cylinder should be zero. It is assumed that the deformation in the cylindrical specimen is homogeneous. The material of the cylinder is chosen such that it provides the necessary elastic restraint to the specimen and deforms elastically during the entire deformation of the specimen; the cylinder must also retain sufficient compliance so as to enable measurement of its deformation during the test. The cylindrical specimen is strained by inserting a plunger into the cavity and displacing it by a loading frame to generate a uniform compressive strain ε_a :

$$\varepsilon_{zz}(r, \theta, z) = \varepsilon_a. \quad (4)$$

The cylindrical polar coordinate system used is shown in Figure 5. The corresponding axial component of stress, $\sigma_{zz}(r, \theta, z) = \sigma_a$, is uniform in the entire specimen and can be measured easily using the load cell in any standard tensile testing machine.

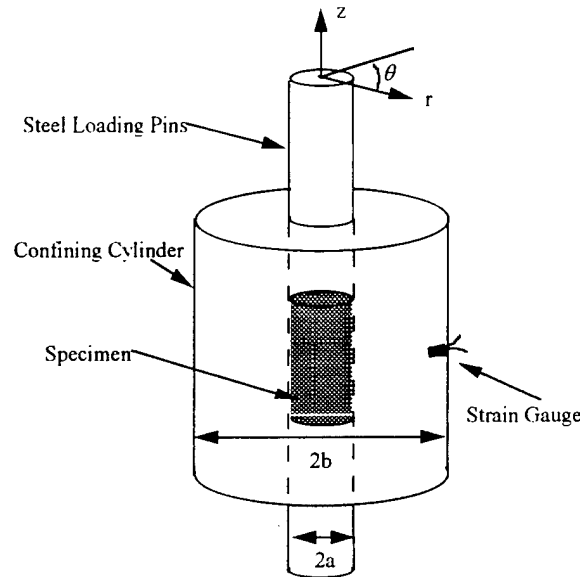


Figure 5. Configuration of the confined compression apparatus for multiaxial characterization.

The confining cylinder provides a restraint against the radial expansion of the specimen, thereby generating a radial pressure on the inner surface of the confining cylinder. The continuity condition on the lateral surfaces of the confining cylinder and specimen may be written as follows: $\sigma_{rr}(a) = \sigma_{rr}^c(a)$ if and only if $u_r(a) = u_r^c(a) > 0$ and $\sigma_{rr}(a) = 0$ otherwise¹. The main idea of this type of constraint is to provide stability to the deformation; in the absence of this elastic restraint, barreling deformations can and do develop. Note that the radial pressure may also be provided by performing the test in a liquid under high pressure; there are a number of experiments in the literature that deal with the response of materials under hydrostatic pressure, beginning with the work of Bridgman (1964). However, hydrostatic pressure from a liquid medium does not stabilize the deformation; in other words, the hydrostatic pressure acts on the lateral surfaces of

¹ Due to the symmetry and uniformity of the fields, only the r dependence is explicitly indicated. The superscript c denotes the confining cylinder.

the cylinder regardless of whether the $u_r(a)$ is greater than zero or not and hence, does not prevent the barreling instability in the compression specimen. On the other hand, the confined compression configuration that is suggested here ensures that the cylindrical deformation is stable. The constraint imposed by the confining cylinder is characterized by the quantities $\sigma_{rr}^c(a)$ and $u_r^c(a)$, and is fully determined by the geometry and material properties of the cylinder. If the hoop strain, $\varepsilon_{\theta\theta}^c(b) \equiv \varepsilon_h$, at the outer surface of the confining steel cylinder is measured using a strain gauge, then, the radial component of displacement and stress at the inner surface of the confining cylinder can be calculated in terms of the measured hoop strain from the Lamé solution (see Timoshenko and Goodier, 1934):

$$u_r^c(a) = \frac{\varepsilon_h}{2} \left[(1 - \nu_c)a + (1 + \nu_c)\frac{b^2}{a} \right] \quad (5)$$

$$\sigma_{rr}^c(a) = -\frac{b^2 - a^2}{2a^2} E_c \varepsilon_h, \quad (6)$$

E_c and ν_c are the modulus of elasticity and Poisson's ratio of the confining cylinder respectively. Since the confining cylinder is free to deform in the axial direction, σ_{zz}^c is taken to be zero and the Lamé solution for plane stress is used in the above equations. Note that the above evaluation of the constraint assumes complete elastic deformation of the confining cylinder, which must be ensured through proper choice of material and geometry for the confining cylinder. This is not strictly necessary; in fact, allowing the confining cylinder to become plastic will provide a way of altering the confining pressure, but will also necessitate a new confining cylinder for each specimen. As discussed above, continuity conditions at the interface between the confining cylinder and the specimen require that the radial component of displacement and stress be equal. Thus, equations (5) and (6) are also the corresponding displacement and stress components in the specimen at $r = a$. Note that the contact is assumed to be frictionless; this can be accomplished by suitable surface finish on the contacting surfaces, through proper lubrication and by minimizing the length of the specimen. For the axisymmetric,

homogeneous deformation the strain displacement relations imply that $\varepsilon_{rr}(a) = \varepsilon_{\theta\theta}(a)$; furthermore, equilibrium equations require that the radial and hoop stress components be equal: $\sigma_{rr}(a) = \sigma_{\theta\theta}(a)$. Thus, the complete state of stress and strain in the cylindrical specimen can be determined from the experimental measurements of the axial strain, ε_a , the axial stress, σ_a , and the hoop strain in the confining cylinder, ε_h . The state of strain and stress in the specimen is homogeneous and is given below in terms of these measured quantities:

$$\begin{aligned}\varepsilon_{rr} = \varepsilon_{\theta\theta} &= \frac{\varepsilon_h}{2} \left[(1 - \nu_c) + (1 + \nu_c) \frac{b^2}{a^2} \right] \\ \varepsilon_{zz} = \varepsilon_a &\cdots \text{imposed by the loading frame and measured} \\ \sigma_{rr} = \sigma_{\theta\theta} &= -\frac{(b/a)^2 - 1}{2} E_c \varepsilon_h \\ \sigma_{zz} = \sigma_a &\cdots \text{measured using a load cell}\end{aligned}\tag{7}$$

Thus, in this experimental configuration the measurements provide a complete determination of the stress components $\sigma_{rr} = \sigma_{\theta\theta}$ and σ_{zz} as well as the corresponding strain components $\varepsilon_{rr} = \varepsilon_{\theta\theta}$ and ε_{zz} without invoking any description of the constitutive behavior of the specimen material! Since these are the principal components of stress and strain, these measurements enable a simple characterization of the constitutive response of the material. This technique was developed in an earlier work and has been quite useful in characterizing the mechanical response of polymers under multiaxial loading (Ravi-Chandar and Ma, 2000)

This configuration provides a confining compression for the polyetherether ketoone (PEEK) specimens. By altering the geometry and material of the confining cylinder, the confinement can be varied. our recent experiments have shown that under confined compression, PEEK can sustain a very high shear stress level. The plot below indicates the axial stress vs. axial strain variation; while the unconfined PEEK exhibits shear yielding at about 25 ksi, the confined specimen (in two repeat trials) is shown to be capable of sustaining a much higher level of compression. The enhancement in the

capacity of PEEK depends on the level of the confinement; in the example shown the confinement was unreasonably high (about 70 ksi), but realistic levels of about 30 ksi can be obtained by suitably altering the microstructure of the composite. We are working on translating this idea to the design and fabrication of fiber composites by generating such compression during processing. This is anticipated to lead to a much higher tensile strength in the composite.

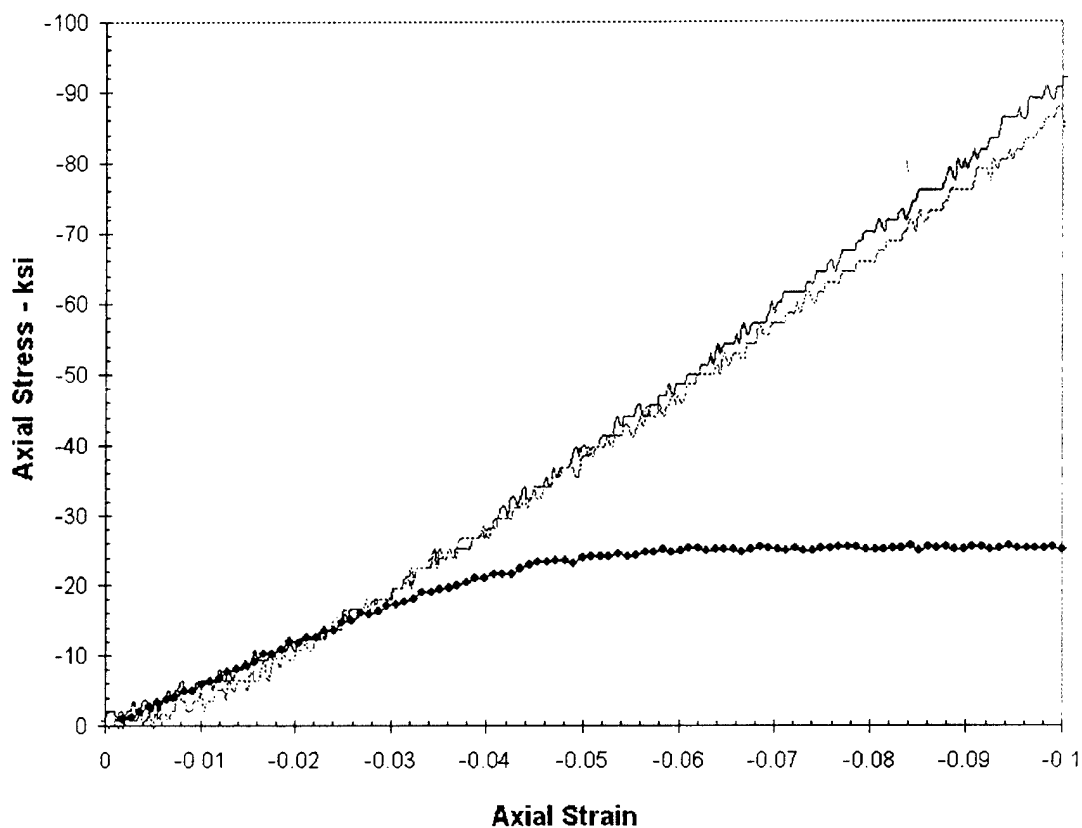


Figure 6. Variation of the axial stress with axial strain for PEEK uniaxial and confined compression tests.

LISTING OF PUBLICATIONS UNDER THIS PROJECT

1. T. Fossier, K. Ravi-Chandar and K.W. White, Development of the digital image correlation method for low strain amplitude measurement, submitted to *Experimental Mechanics*, June 2001.
2. R. Wang and K. Ravi-Chandar, Mechanical behavior of PEEK under multiaxial compression, under preparation.

LISTING OF PUBLICATIONS UNDER THIS PROJECT

Renjun Wang, Graduate Student (now with the PI at the University of Texas at Austin)

BIBLIOGRAPHY

Bridgman, P.W., 1964, **Studies in large plastic flow and fracture**, Harvard University Press.

Peters, W.H. & Ranson, W.F. Digital Imaging Techniques in Experimental Stress Analysis. *Optical Engineering* **21**, 427-432 (1980).

Ravi-Chandar, K. and Ma, Z, Inelastic deformation in polymers under multiaxial loading, *Mechanics of Time-Dependent Materials*, **4**, (2000), 333-357.

Sutton M.A., Turner J.L., Bruck H.A. & Chae T.A. Full Field Representation of Discretely Sampled Surface Deformation for Displacement and Strain Analysis. *Experimental Mechanics* **31**, 168-177 (1991).

Timoshenko, S.P., and J. N. Goodier, 1934 *Theory of Elasticity*, McGraw Hill, New York.

Vendroux, G. & Knauss, W.G. Submicron deformation field measurements: Part 2. Improved digital image correlation. *Experimental Mechanics* **38**, 85-92 (1998).